

RESEARCH

Open Access



Developing and validating a predictive model for all-cause mortality in patients with metabolic dysfunction-associated steatotic liver disease

Fan Zhang^{1,2,5}, Longgen Liu^{3,5} and Wenjian Li^{4,5*}

Abstract

Objective This study aimed to construct a scientific, accurate, and readily applicable clinical all-cause mortality prediction model for patients with metabolic dysfunction-associated steatotic liver disease (MASLD) to enhance the efficiency of disease management and improve patient prognosis.

Methods This study was a retrospective cohort study based on the National Health and Nutrition Examination Survey database. The 17,861 participants diagnosed with MASLD were randomly assigned to either a training cohort (n = 12,503) or a validation cohort (n = 5358). Potential predictors were subjected to LASSO regression analysis, and independent risk factors were subsequently identified through multivariate Cox regression analysis. An all-cause mortality prediction model was constructed based on the significant predictors, and a nomogram was generated to illustrate the survival probability of patients at various time points. The model's performance was evaluated using receiver operating characteristic (ROC), calibration, and decision curve analysis (DCA) curves.

Results A multiple Cox regression analysis identified several independent predictors significantly influencing all-cause mortality in patients with MASLD. These included gender, age, smoking status, hypertension, red blood cell count, albumin, glutamyl transpeptidase, glycosylated hemoglobin, and creatinine. The constructed predictive model demonstrated high accuracy in the training and validation cohorts, with AUC values approaching 0.85 at 3, 5, and 10 years, respectively. Calibration and DCA curves were employed to verify the stability and generalizability of the model.

Conclusions We successfully constructed and validated an all-cause mortality prediction model for MASLD patients. This model provides a powerful tool for clinical risk assessment and treatment decision-making.

Keywords Metabolic dysfunction-associated steatotic liver disease, All-cause mortality, Predictive modeling, NHANES, Cox regression analysis

*Correspondence:

Wenjian Li

bolite@163.com

Full list of author information is available at the end of the article



© The Author(s) 2025. **Open Access** This article is licensed under a Creative Commons Attribution-NonCommercial-NoDerivatives 4.0 International License, which permits any non-commercial use, sharing, distribution and reproduction in any medium or format, as long as you give appropriate credit to the original author(s) and the source, provide a link to the Creative Commons licence, and indicate if you modified the licensed material. You do not have permission under this licence to share adapted material derived from this article or parts of it. The images or other third party material in this article are included in the article's Creative Commons licence, unless indicated otherwise in a credit line to the material. If material is not included in the article's Creative Commons licence and your intended use is not permitted by statutory regulation or exceeds the permitted use, you will need to obtain permission directly from the copyright holder. To view a copy of this licence, visit <http://creativecommons.org/licenses/by-nc-nd/4.0/>.

Introduction

In recent years, the global rise in obesity and metabolic syndrome has led to an increase in cases of metabolic dysfunction-associated steatotic liver disease (MASLD). This liver disease has become a significant public health concern [1–5]. MASLD, frequently designated as a subset of nonalcoholic fatty liver disease (NAFLD), denotes explicitly those forms of fatty liver disease that are intimately associated with the metabolic syndrome [6]. This disease affects the liver's normal function and leads to abnormal fat deposition in hepatocytes. Furthermore, it may exacerbate the patient's overall metabolic disorder through complex pathophysiological mechanisms, such as insulin resistance, chronic inflammation, and oxidative stress. This, in turn, increases the risk of cardiovascular disease, type 2 diabetes, malignant tumors, and many other chronic diseases [6–10].

As our comprehension of MASLD deepens, it has become increasingly evident that diagnosing MASLD through liver biopsy or imaging alone is insufficient for meeting the needs of early identification, risk assessment, and intervention and treatment in clinical practice. It is, therefore, of great significance to construct a scientific, accurate, and readily applicable clinical all-cause mortality prediction model for MASLD patients to improve the efficiency of disease management and prognosis.

Nevertheless, the current research on the long-term prognostic assessment of MASLD patients still presents numerous challenges. On the one hand, the pathogenesis of MASLD is complex and involves genetic, environmental, lifestyle, and other factors, making its predictive assessment particularly challenging [11–14]. In contrast, extant studies have substantiated the correlation between a range of indicators and mortality in MASLD, encompassing, but not limited to, triglyceride-glucose-related parameters [9, 15], the systemic inflammation response index [16], cardiometabolic risk factors [17], and hematological biomarkers of inflammation [18]. However, it is essential to note that while the correlation between these indices and MASLD mortality has been confirmed, they all demonstrated some limitations regarding predictive accuracy. In light of these considerations, constructing a prediction model that can be widely applied to different populations and accurately predict all-cause mortality in patients with MASLD has become a significant focus of current medical research.

In this study, we first screened patients who met the diagnostic criteria for MASLD through the National Health and Nutrition Examination Survey (NHANES) database and subsequently constructed an all-cause mortality prediction model based on baseline data for this population. A multivariate Cox regression analysis was employed to construct a prediction model that integrates

several factors, including patient demographic characteristics, lifestyle, co-morbidities, anthropometrics, and laboratory test indicators. The establishment of this model facilitates a more comprehensive understanding of the pathogenesis of MASLD and its impact on patient prognosis. Furthermore, it provides substantial support for risk assessment, treatment decision-making, and prognosis management of MASLD patients in clinical practice.

Materials and methods

Study population

This study was a retrospective cohort study based on the NHANES database. The data utilized in this study were obtained from the NHANES database, spanning 1999 to 2018. This database contains the results of cross-sectional surveys conducted every two years by the Centers for Disease Control and Prevention (CDC). The research protocol of the NHANES project adhered strictly to the guidelines set forth by the Ethics Review Committee of the National Center for Health Statistics (NCHS), and all participants were required to sign an informed consent form. During data analysis, the NIH policy regulations were adhered to. Given the anonymity and non-direct contact nature of the data, it was used directly in the study without requiring additional ethical review because it was not identifiable. To ensure the highest study design and reporting quality, the study was conducted according to the standards outlined in the Strengthening the Reporting of Observational Studies in Epidemiology (STROBE) statement.

At the study's outset, a sample population was selected from ten consecutive survey cycles, comprising 101,316 participants. To guarantee the precision and applicability of the study outcomes, we employed rigorous data cleansing and exclusion protocols to remove ineligible participants, including those under the age of 20, pregnant women, individuals with incomplete data sets (specifically lacking information on essential indicators for calculating the fatty liver index (FLI), demographic characteristics, chronic disease status, survival follow-up, and select biochemical data), and non-MASLD patients. Following applying the above screening criteria, 17,861 participants were identified as eligible for inclusion in the analysis of this study. These participants were then randomly assigned to a training and validation cohort in a ratio of 7:3 (Fig. 1).

Data collection

The data utilized in this study were obtained from the NHANES dataset. The data set included information on gender, age, race, education, marital status, family poverty-to-income ratio (PIR), smoking status, drinking status, physical activity level, diabetes, hypertension,

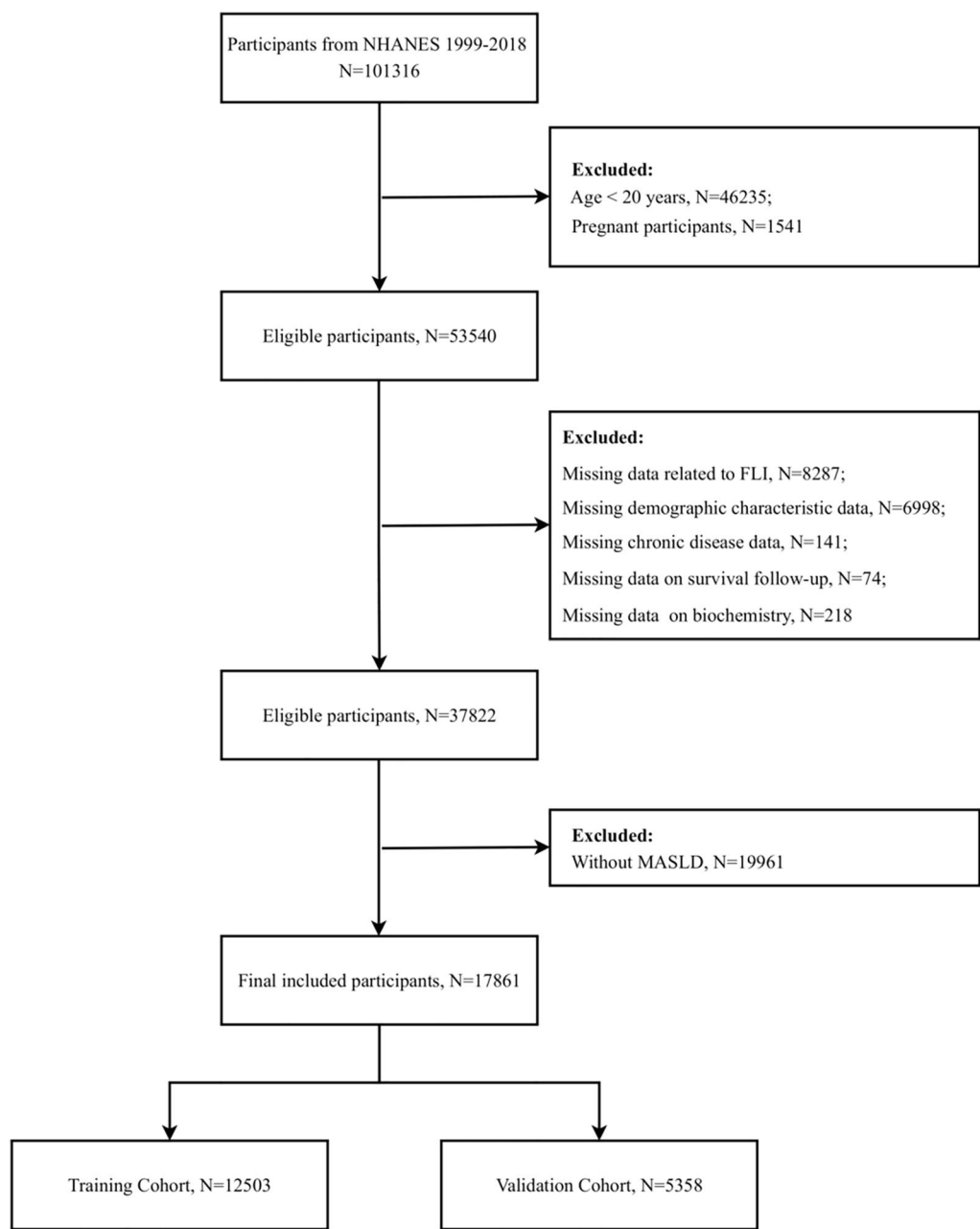


Fig. 1 Participant screening flowchart. *FLI* fatty liver index, *MASLD* metabolic dysfunction-associated steatotic liver disease

body mass index (BMI), waist circumference (WC), white blood cell count (WBC), red blood cell count (RBC), platelet count, hemoglobin, albumin, total bilirubin, aspartate transferase (AST), alanine transferase (ALT), gamma-glutamyl transpeptidase (GGT), fasting plasma glucose (FPG), glycosylated hemoglobin (HbA1c), total cholesterol (TC), triglycerides (TG), high-density lipoprotein cholesterol (HDL-c), creatinine, uric acid, and blood urea nitrogen (BUN).

For racial categorization, participants were subdivided into the following categories: Mexican American, non-Hispanic White, non-Hispanic Black, and other race. Educational attainment was based on participants' self-reported highest level of education. It was categorized into three categories: less than high school (did not complete 9th grade), high school diploma (graduated from grades 9–12), and more than high school (completed more than 12th grade) [19]. To examine the influence

of family structure variables, marital status was dichotomized into cohabitation and solitude. To assess the family's economic status, our approach was to base our evaluation on the PIR criterion officially defined by the U.S. government [20]. Standardized assessment methods were employed to ascertain smoking and drinking habits. The status of the participant smoking was determined by the number of cigarettes smoked more than 100 in the course of the participant's lifetime, as well as the current status of the participant as a smoker [21]. Alcohol consumption was assessed using a question regarding the consumption of at least 12 alcoholic beverages of any type in the past year [22]. Physical activity was categorized according to the NHANES metabolic equivalent (MET) criteria: vigorous (≥ 6.0 METs), moderate (3.0–5.9 METs), and inactive (< 3.0 METs), with definitions referenced to the NHANES Physical Activity Questionnaire guidelines. Diagnosis of diabetes was based on one of the following criteria: a medical professional diagnosis, an FPG level of ≥ 126 mg/dL, an HbA1c level of $\geq 6.5\%$, or glucose-lowering therapy. Hypertension was diagnosed based on whether participants had been informed by a medical professional that they had hypertension or were currently taking medication prescribed for hypertension.

MASLD assessment

In the initial stages of MASLD, the disease is typically identified by an abnormal fat accumulation within the liver tissue. In the absence of data from ultrasound assessments of hepatic steatosis and transient elastography of the liver over multiple follow-up cycles, the evaluation of MASLD status is primarily based on the calculation of the FLI [23], which is calculated using the following formula:

$$FLI = \frac{(e^{0.953 \times \ln(TG) + 0.139 \times BMI + 0.718 \times \ln(GGT) + 0.053 \times WC - 15.745})}{(1 + e^{0.953 \times \ln(TG) + 0.139 \times BMI + 0.718 \times \ln(GGT) + 0.053 \times WC - 15.745})} \times 100$$

According to the findings of previous studies, individuals with FLI values below 60 are deemed at low risk for hepatic steatosis [23]. In contrast, individuals with FLI values at or above 60 are considered to be at high risk for hepatic steatosis and are accordingly diagnosed [24]. Furthermore, a diagnosis of MASLD was confirmed if any of the following five cardiometabolic criteria were met: (1) $BMI \geq 25$ kg/m², or $WC \geq 94$ cm in men and ≥ 80 cm in women; (2) $FPG \geq 100$ mg/dL, or 2-h post-load blood glucose level ≥ 140 mg/dL, or $HbA1c \geq 5.7\%$, or diagnosed diabetes mellitus (DM), or receiving glucose-lowering therapy for DM; (3) blood pressure $\geq 130/85$ mmHg, or being treated with antihypertensive medication; (4) $TG \geq 150$ mg/dL, or being treated with lipid-lowering therapy; and (5) HDL-c level < 40 mg/dL in men and

< 50 mg/dL in women, or being treated with lipid-lowering therapy [6].

Mortality assessment

The principal objective of this study was to ascertain the incidence of mortality in patients with MASLD. The term "all-cause mortality" was used to describe deaths from heart disease, malignant neoplasms, and all other causes. The mortality data for the follow-up population were obtained from the NHANES Public Use-Related Mortality File (as of December 31, 2019). This file is correlated to the NCHS and the National Death Index (NDI) through a probabilistic matching algorithm. The follow-up period was calculated from the initial interview to the date of the patient's death or December 31, 2019 [25].

Statistical analysis

To verify the normality of continuous variables, the Kolmogorov–Smirnov test was implemented. By the outcomes of the normality test, the mean \pm standard deviation or the median (in conjunction with the 25th and 75th percentile) were selected for descriptive analysis. To ascertain the distributional characteristics of the variables in question, we employed the Student's t-test or rank sum test, which enabled us to identify and compare differences between the various groups. A frequency and percentage table was provided for categorical variables, and the chi-square test was used to analyze differences between groups.

In the training cohort, we employed the least absolute shrinkage and selection operator (LASSO) Cox regression analysis method for multivariate analysis to identify independent risk factors. Subsequently, we further employed multivariate Cox regression analysis to refine the independent predictors and constructed a nomogram of predicted all-cause mortality. To assess the efficacy of this nomogram in the training cohort and validation cohort, we employed receiver operating characteristic (ROC) and calibration curves, respectively. The area under the ROC curve (AUC) ranged from 0.5 (indicating no discriminatory power) to 1 (indicating full discriminatory power). Furthermore, decision curve analysis (DCA) curves were conducted to ascertain the predicted net benefit threshold. To evaluate the cumulative incidence of mortality across different subgroups (e.g., gender, smoking status, and hypertension), we employed the Kaplan–Meier method and log-rank tests.

In all statistical analyses, we adhered to the principle of two-sided tests and considered *P* values less than 0.05 to be statistically significant. All data analysis was conducted with the assistance of R 4.4.0 software (provided by the R Foundation at <http://www.R-project.org>) and SPSS version 23.0 (IBM Corporation, Armonk,

NY, USA). Graphic presentations were generated using GraphPad Prism version 9.0 (GraphPad Software, USA).

Results

Baseline characteristics of participants

This study analyzed the participants' demographic and baseline clinical characteristics. 12,503 participants were included in the training cohort, and 5358 were included in the validation cohort. The gender distribution indicated that 55.7% of the training and 55.8% of the validation cohorts were male, with no statistically significant difference ($P=0.860$). The median age was 52 years for the training cohort and 53 years for the validation cohort. A comparison of age distributions revealed no statistically significant difference between the two groups ($P=0.761$). Regarding racial composition, the most significant proportion was that of non-Hispanic whites, representing 45.9% of the training cohort and 46.4% of the validation cohort. No significant differences were observed in the racial distributions ($P=0.438$). No significant differences were observed between the two groups regarding education level, marital status, family PIR, smoking, drinking habits, physical activity level, prevalence of DM, and hypertension (all $P>0.05$). Furthermore, no significant differences were observed in the median values of anthropometric and biomarker variables between the two groups, including BMI, WC, WBC, RBC, platelet, hemoglobin, albumin, total bilirubin, AST, ALT, GGT, FPG, TC, TG, HDL-c, creatinine, uric acid, and BUN (all $P>0.05$) (Table 1).

LASSO regression

In this study, we employed LASSO regression to select features. The following features were included in the analysis: gender, age, race, education, marital status, family PIR, smoking status, alcohol status, physical activity level, diabetes, hypertension, BMI, WC, WBC, RBC, platelet, hemoglobin, albumin, total bilirubin, AST, ALT, GGT, FPG, HbA1c, TC, TG, HDL-c, creatinine, uric acid, and BUN. These variables were evaluated using LASSO regression. Figure 2A depicts the LASSO regression coefficient profiles, which illustrate the process of model variable selection by displaying the alterations in the coefficients of the variables at varying λ values. As the value of λ increases, the regression coefficients of some variables gradually approach zero, thereby achieving a sparse selection of variables. Figure 2B depicts the cross-validation error plot of the LASSO regression model, which is utilized to ascertain the optimal model complexity by calculating the cross-validation error at varying λ values. As illustrated in the figure, examining the model deviation reveals a pattern of decreasing and then increasing as the λ value increases. This suggests the

existence of an optimal λ value that enables the model to perform optimally in cross-validation. Specifically, the model performs better when the deviation corresponding to the value of λ decreases from 11.5 to approximately 9.0. However, increasing the value of λ leads to an increase in the deviation, resulting in a decline in the model's performance. In conclusion, the results of the LASSO regression demonstrated that a total of 19 variables were identified as potential predictors, including gender, age, race, marital status, family PIR, smoking, physical activity, diabetes, hypertension, WC, RBC, albumin, AST, GGT, FPG, HbA1c, creatinine, uric acid, and BUN.

Multivariate Cox regression analysis

Following a multivariate Cox regression analysis of 19 variables that had been screened by LASSO regression, it was determined that gender, age, smoking status, hypertension, RBC, albumin, GGT, HbA1c, and creatinine levels were significant factors influencing the risk of death in patients. Specifically, the risk of death was lower in females than in males (HR=0.70, 95% CI: 0.63–0.77, $P<0.001$). An increase in age was associated with an elevated risk of mortality (HR=1.08, 95% CI: 1.08–1.09, $P<0.001$). Conversely, smokers and hypertensive patients exhibited a markedly elevated risk of mortality compared to non-smokers and non-hypertensive patients (HR=1.47, 95% CI: 1.34–1.62, $P<0.001$; HR=1.26, 95% CI: 1.15–1.39, $P<0.001$). It is noteworthy that lower RBC counts were associated with an elevated risk of mortality (HR=0.77, 95% CI: 0.70–0.85, $P<0.001$), while lower albumin levels similarly predicted an increased risk of mortality (HR=0.50, 95% CI: 0.43–0.58, $P<0.001$). Furthermore, elevated GGT, HbA1c, and creatinine levels were all found to increase the risk of death significantly (HR=1.01, 95% CI: 1.01–1.01, $P<0.001$; HR=1.14, 95% CI: 1.10–1.17, $P<0.001$; HR=1.16, 95% CI: 1.12–1.21, $P<0.001$) (Table 2).

Constructing the nomogram

The multivariate Cox regression analysis results were used to construct a final model containing nine independent predictors. These results designed a concise and practical nomogram, as shown in Fig. 3. The nomogram was designed to illustrate the probability of survival for patients with MASLD at specified time points, namely 3, 5, and 10 years. To construct this graph, a point system was employed that incorporated gender, age, smoking status, hypertension, RBC, albumin, GGT, HbA1c, and creatinine levels as predictors of survival. In particular, each predictor was assigned a score independently, and the resulting scores were summed to calculate the probability of patient survival at each time point. The range of

Table 1 Patient demographics and baseline characteristics

Variables	Cohort		P
	Training cohort, N = 12,503	Validation cohort, N = 5358	
Gender, n (%)			0.860
Male	6964 (55.7%)	2992 (55.8%)	
Female	5539 (44.3%)	2366 (44.2%)	
Age (years)	52 (39, 65)	53 (40, 65)	0.761
Race, n (%)			0.438
Mexican American	2469 (19.7%)	1087 (20.3%)	
Non-Hispanic White	5738 (45.9%)	2484 (46.4%)	
Non-Hispanic Black	2531 (20.2%)	1076 (20.1%)	
Other Race	1765 (14.1%)	711 (13.3%)	
Education level, n (%)			0.763
Less than 9th grade	1493 (11.9%)	660 (12.3%)	
9–12th grade	5015 (40.1%)	2148 (40.1%)	
More than 12th grade	5995 (47.9%)	2550 (47.6%)	
Marital Status, n (%)			0.593
Cohabitation	7898 (63.2%)	3362 (62.7%)	
Solitude	4605 (36.8%)	1996 (37.3%)	
Family PIR	2.10 (1.13, 3.96)	2.13 (1.16, 4.01)	0.354
Smoking, n (%)			0.339
No	6154 (49.2%)	2679 (50.0%)	
Yes	6349 (50.8%)	2679 (50.0%)	
Alcohol, n (%)			0.087
No	3852 (30.8%)	1720 (32.1%)	
Yes	8651 (69.2%)	3638 (67.9%)	
Physical activity, n (%)			0.308
Inactive	4013 (32.1%)	1731 (32.3%)	
Moderate	4658 (37.3%)	2044 (38.1%)	
Vigorous	3832 (30.6%)	1583 (29.5%)	
Diabetes, n (%)			0.579
No	9165 (73.3%)	3949 (73.7%)	
Yes	3338 (26.7%)	1409 (26.3%)	
Hypertension, n (%)			0.785
No	6655 (53.2%)	2840 (53.0%)	
Yes	5848 (46.8%)	2518 (47.0%)	
BMI (kg/m ²)	32.5 (29.5, 36.6)	32.5 (29.4, 36.6)	0.873
WC (cm)	109 (102, 118)	109 (103, 118)	0.444
WBC (10 ³ cells/ μ L)	7.30 (6.10, 8.80)	7.40 (6.10, 8.80)	0.371
RBC (million cells/ μ L)	4.78 (4.45, 5.11)	4.78 (4.43, 5.10)	0.373
Platelet (10 ³ cells/ μ L)	248 (209, 294)	248 (209, 295)	0.984
Hemoglobin (g/dL)	14.40 (13.40, 15.40)	14.40 (13.40, 15.50)	0.998
Albumin (g/dL)	4.20 (4.00, 4.40)	4.20 (4.00, 4.40)	0.600
Total Bilirubin (mg/dL)	0.60 (0.50, 0.90)	0.60 (0.50, 0.90)	0.283
AST (U/L)	24 (20, 29)	24 (20, 29)	0.503
ALT (U/L)	24 (18, 34)	24 (18, 34)	0.477
GGT (IU/L)	27 (19, 42)	27 (19, 41)	0.260
FPG (mg/dL)	97 (88, 111)	97 (88, 111)	0.753
HbA1c (%)	5.60 (5.30, 6.10)	5.60 (5.30, 6.10)	0.192
TC (mg/dL)	197 (171, 226)	198 (171, 227)	0.980
TG (mg/dL)	163 (114, 242)	166 (114, 244)	0.457

Table 1 (continued)

Variables	Cohort		P
	Training cohort, N = 12,503	Validation cohort, N = 5358	
HDL-c (mg/dL)	45 (38, 53)	44 (38, 53)	0.776
Creatinine (mg/dL)	0.89 (0.73, 1.02)	0.89 (0.73, 1.02)	0.872
Uric acid (mg/dL)	5.90 (4.90, 6.90)	5.90 (5.00, 6.80)	0.464
BUN (mg/dL)	13.0 (10.0, 17.0)	13.0 (10.0, 16.0)	0.205

Data are shown as median (25th, 75th percentiles) or percentages, $p < 0.05$ considered statistically significant

PIR poverty-to-income ratio, BMI body mass index, WC waist circumference, WBC white blood cell count, RBC red blood cell count, FPG fasting plasma-glucose, AST aspartate aminotransferase, ALT alanine transaminase, GGT gamma-glutamyl transferase, HbA1c hemoglobin A1c, TC total cholesterol, TG triglyceride, HDL-c high density lipoprotein cholesterol, BUN blood urea nitrogen

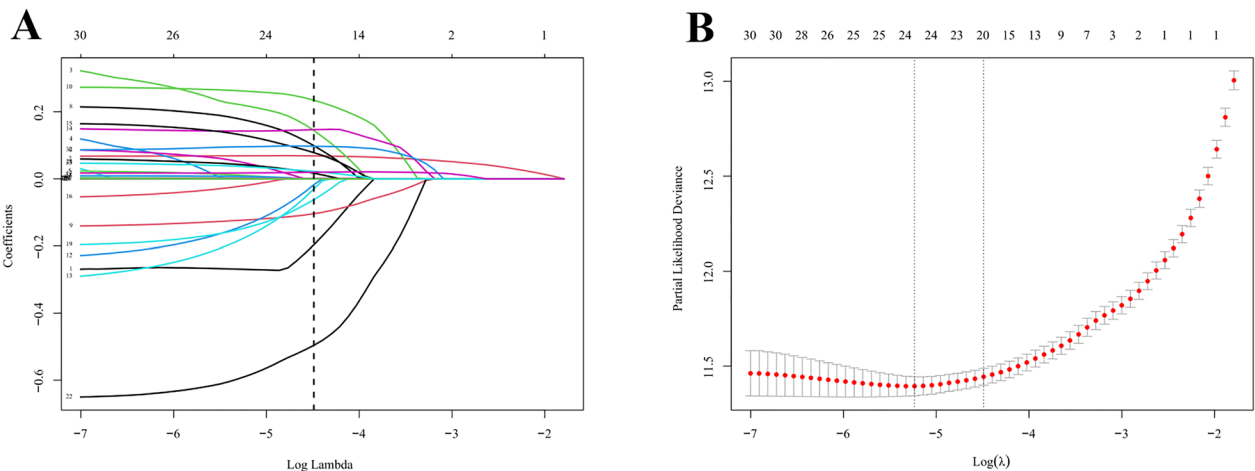


Fig. 2 LASSO regression for variable selection in MASLD patients to reduce multicollinearity. **A** The coefficient profiles of predictors showcase the LASSO coefficient profiles for the 30 evaluated predictors. A coefficient profile plot against the logarithmic λ sequence $[\log(\lambda)]$ is displayed. This plot helps to understand how each predictor's influence varies with changes in the λ value, illustrating the dynamic nature of variable selection in the LASSO model. **B** Tuning parameter (λ) selection using tenfold cross-validation to show the process of λ optimization in the LASSO model to balance model complexity and predictive accuracy. The dotted vertical line indicates the chosen λ value, which resulted in the selection of 19 significant predictors with non-zero coefficients

survival probability was set from 0.01 to 0.99, with higher values indicating more favorable survival outcomes. The nomogram demonstrates the correlation between these variables and survival outcomes clearly and comprehensively, thereby providing substantial support for clinical decision-making and risk assessment.

ROC curves, calibration curves, and DCA curves

This study presented the ROC curves of the training and validation cohorts to assess the developed model's predictive performance. Figure 4A depicts the ROC curves of the training cohort, whose 3-, 5-, and 10-year AUCs were 0.813, 0.826, and 0.848, respectively. These results indicate that the model had high accuracy in predicting patients' survival and demonstrated an inevitable trend of improvement over time. Figure 4B depicts the ROC curves of the validation cohort, with AUC values of 0.825, 0.839, and 0.845 at 3, 5, and 10 years, respectively. The

validation cohort exhibits slightly higher AUC values at the same time points than the training cohort, indicating that the model has a superior capacity for generalization to an independent validation set. This finding reinforces the model's reliability and applicability in predicting the probability of long-term patient survival.

Furthermore, the calibration curves for the ROC curve analysis on 3-, 5-, and 10-year survival prediction for both the training and validation cohorts are presented. As illustrated in Fig. 5, the calibration curves of the model on 3-, 5-, and 10-year survival prediction for both the training and validation cohorts exhibit a high degree of accuracy, with a fit to the ideal curve (i.e., the predicted probability is equal to the diagonal of the actual likelihood of occurrence). This indicates that the model can accurately predict survival probabilities at different time points in both the training dataset and

Table 2 Results of multivariate cox regression for training cohort

Variables	N	Death	HR	95% CI	P
Gender					
Male	6964	1201	–	–	
Female	5539	791	0.70	0.63, 0.77	<0.001
Age	12,503	1992	1.08	1.08, 1.09	<0.001
Smoking					
No	6154	718	–	–	
Yes	6349	1274	1.47	1.34, 1.62	<0.001
Hypertension					
No	6655	680	–	–	
Yes	5848	1312	1.26	1.15, 1.39	<0.001
RBC	12,503	1992	0.77	0.70, 0.85	<0.001
Albumin	12,503	1992	0.50	0.43, 0.58	<0.001
GGT	12,503	1992	1.00	1.00, 1.00	<0.001
HbA1c	12,503	1992	1.14	1.10, 1.17	<0.001
Creatinine	12,503	1992	1.16	1.12, 1.21	<0.001

HR hazard ratio, CI confidence interval, RBC red blood cell count, GGT gamma-glutamyl transferase

the validation set, thereby demonstrating the stability and generalization ability of the model.

Furthermore, we present the DCA curves derived from the ROC curve analysis of the training cohort compared to the validation cohort concerning 3-, 5-, and 10-year survival prediction. These curve plots aim to assess the model's net benefit in clinical decision-making by comparing the net benefit at different threshold probabilities and the strategy of treating all patients versus not treating any patients. The DCA curves for the training cohort indicate that the net benefit of utilizing the model for decision-making is markedly superior to the "treat all" or "treat none" strategies at various threshold probabilities, particularly within the medium to high threshold range. Similarly, the DCA curves for the validation cohort illustrate the model's efficacy in predicting survival probability. The model exhibited a high net benefit at various time points (3, 5, and 10 years), further substantiating its stability and capacity for generalization (Fig. 6).

Kaplan–Meier survival curve subgroup analysis

In this study, we constructed all-cause mortality survival curves for various subgroups (gender, smoking status, and hypertension status) for the training and validation cohorts. In the gender subgroup, a comparison of

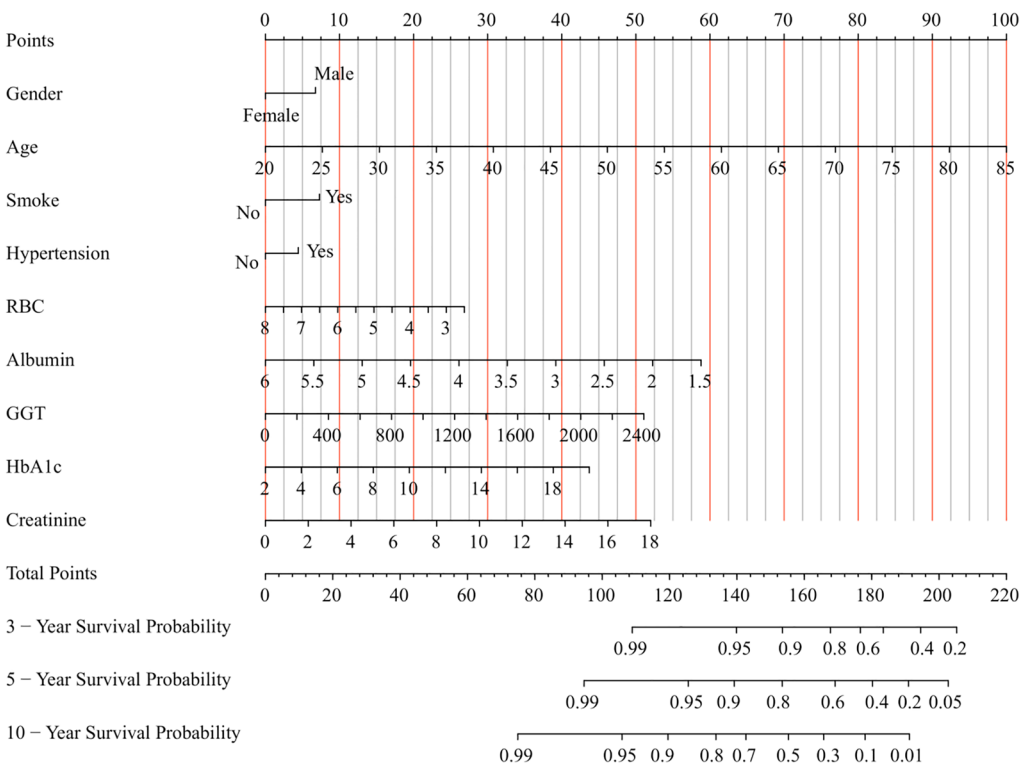


Fig. 3 Nomogram for predicting the probability of survival for patients with MASLD at specific time points, namely 3, 5, and 10 years. Values for each variable are individually plotted and correspond to point values assigned from the point scale (top). A total score was obtained from the values of each index and plotted on the total point scale (bottom), which is used to assign a corresponding value for the predicted rate of the nomogram. RBC red blood cell count, GGT gamma-glutamyl transferase

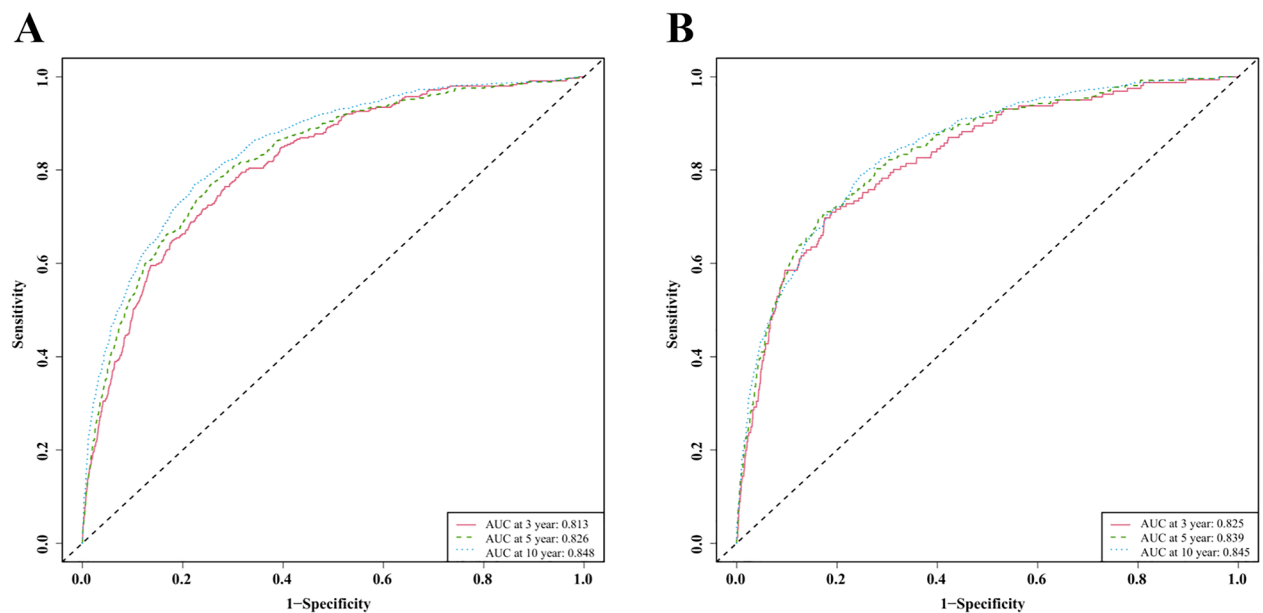


Fig. 4 ROC curves of nomogram in training and validation cohorts. **A** ROC curves of the training cohort at 3, 5, and 10 years; **B** ROC curves of the validation cohort at 3, 5, and 10 years. *ROC* receiver operating characteristic, *AUC* area under the receiver operating characteristic curve

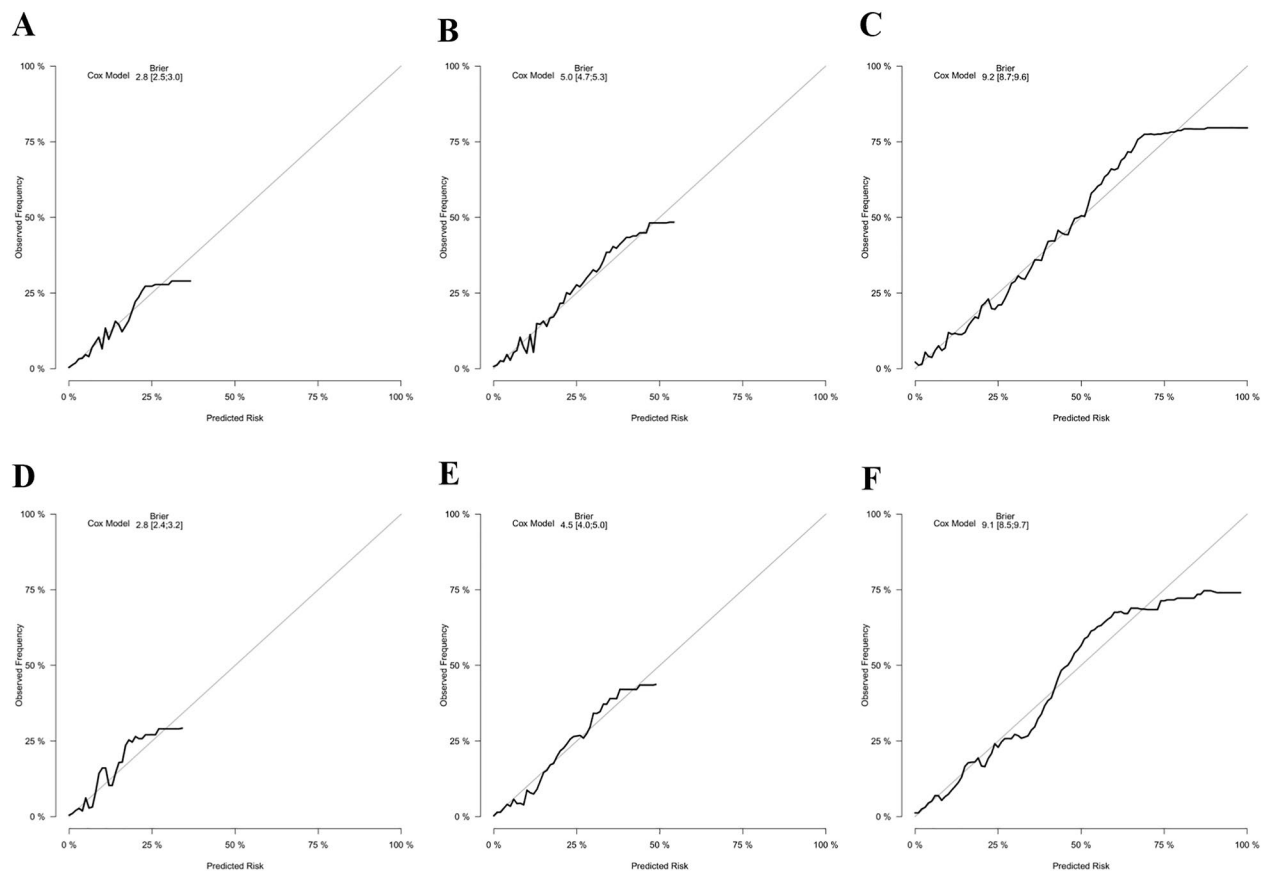


Fig. 5 Calibration curve of the nomogram. This figure presents the calibration curve of the nomogram using data from **A–C** the training cohort and **D–F** the validation cohort

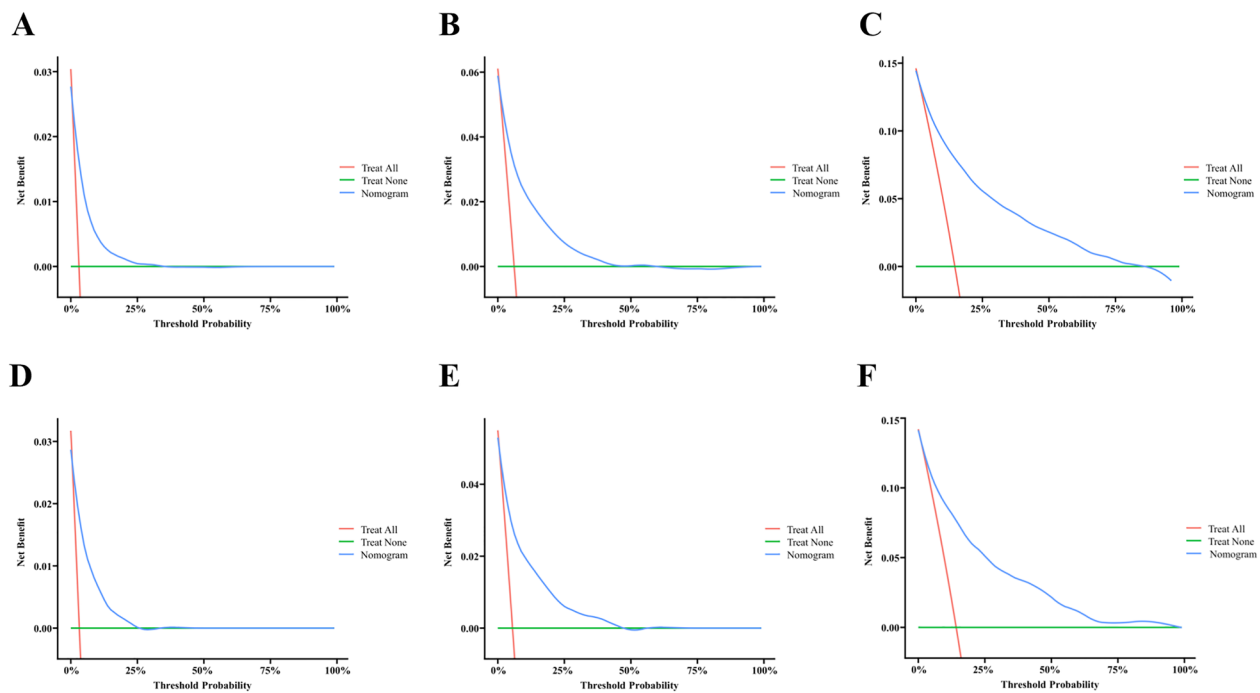


Fig. 6 Evaluation of the clinical benefit of the nomogram. This figure displays the assessment of the clinical benefit of the predictive model using data from **A–C** the training cohort and **D–F** the validation cohort

survival curves between women and men in the training cohort revealed that women exhibited a higher probability of survival. The Log-rank test p-value was less than 0.001, and the HR (95% CI) was 1.201 (1.098–1.314). Similarly, the validation cohort demonstrated a higher probability of survival for women than men, with a log-rank test p-value less than 0.001 and an HR (95% CI) of 1.364 (1.188–1.565). In the subgroup defined by smoking status, the survival curves of smokers versus non-smokers in the training cohort revealed a significantly poorer prognosis for smokers, with a notable decline in the probability of survival over time. The log-rank test p-value was less than 0.001, and the HR (95% CI) was 1.749 (1.596–1.916). The survival curves for smokers in the validation cohort similarly demonstrated a lower probability of survival, consistent with the findings of the training cohort. The log-rank test p-value was again less than 0.001, and the HR (95% CI) was 1.556 (1.357–1.784). In the hypertension subgroup, the probability of survival was lower for individuals with hypertension in the training cohort than for those without hypertension. The log-rank test p-value was less than 0.001, and the HR (95% CI) was 2.599 (2.369–2.852). Similarly, the validation cohort demonstrated a lower probability of survival among individuals with hypertension, with a log-rank test p-value less than 0.001 and an HR (95% CI) of 2.665 (2.312–3.072) (Fig. 7).

Discussion

This study successfully constructed an all-cause mortality prediction model for adult patients with MASLD by comprehensively analyzing substantial data from the NHANES database. The findings revealed significant correlations between key predictors, including gender, age, smoking status, hypertension, RBC, albumin, GGT, HbA1c, and creatinine, and all-cause mortality in patients with MASLD. These findings offer novel insights into the pathophysiological mechanisms of MASLD and provide clinicians with a crucial foundation for evaluating the risk of mortality in patients.

In this study, we employed multivariate Cox regression analysis to screen nine independent predictors that significantly influenced all-cause mortality in patients with MASLD. Among these, albumin, smoking, and creatinine levels exhibited the most substantial influence on all-cause mortality in MASLD patients. Albumin, a vital indicator of hepatic synthetic function, shows a reduced level in cases of impaired hepatic synthetic capacity or malnutrition [26]. Hypoalbuminemia is associated with increased systemic inflammatory response and immune suppression, which may exacerbate metabolic disorders and organ damage in patients with MASLD, thereby increasing the risk of death [27, 28]. Furthermore, hypoalbuminemia may serve as an indicator of hepatic fibrosis progression, which can further affect multi-organ

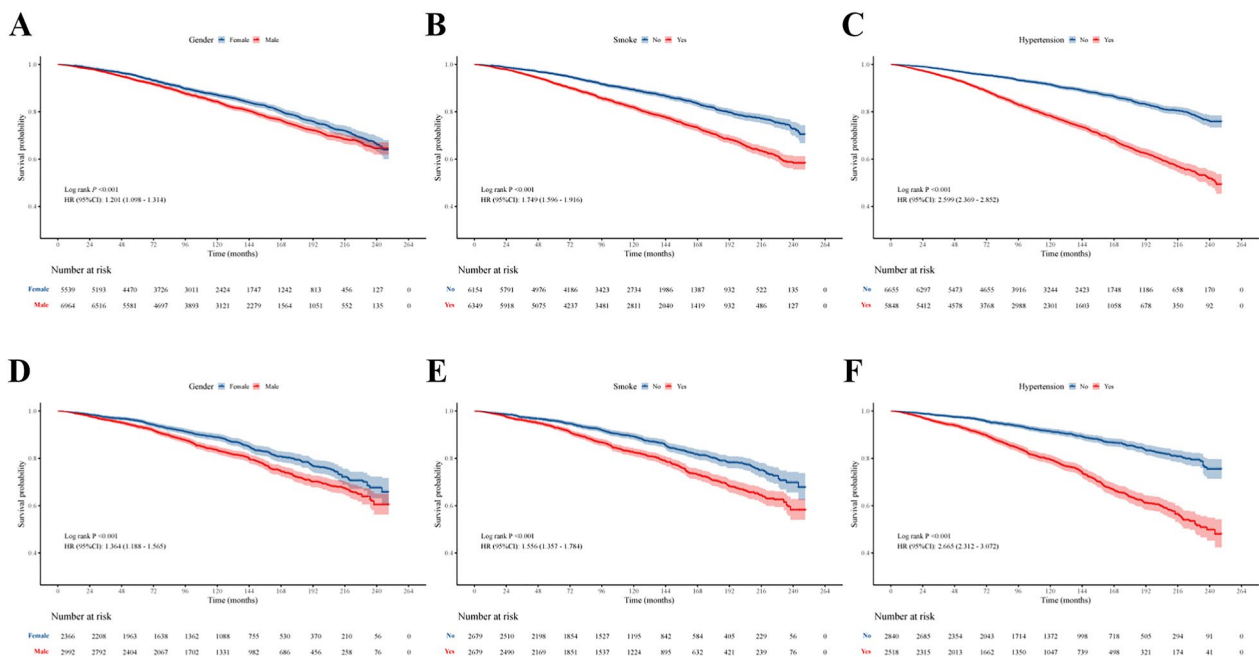


Fig. 7 Kaplan–Meier curves for all-cause mortality stratified by gender (A), smoking status (B), and hypertension status (C) in the training cohort. Kaplan–Meier curves for all-cause mortality stratified by gender (D), smoking status (E), and hypertension status (F) in the validation cohort. In the Kaplan–Meier curves, the population is stratified into two groups and statistical analysis is conducted using the log-rank test

homeostasis [29]. Furthermore, the pathologic process in patients with MASLD is exacerbated by cigarette smoking through multiple pathways. Harmful components of tobacco, such as nicotine, can directly induce oxidative stress and inflammatory responses in hepatocytes, accelerating liver fibrosis [30, 31]. Furthermore, smoking is significantly associated with an increased risk of cardiovascular disease. It may synergize with metabolic abnormalities in MASLD through pro-atherosclerotic and endothelial dysfunction mechanisms, contributing to an elevated risk of cardiac death [32–34]. Furthermore, smoking has been demonstrated to exacerbate insulin resistance, thereby further exacerbating metabolic disorders through epigenetic modulation [35]. Elevated creatinine levels are indicative of renal insufficiency and may reflect systemic metabolic toxin accumulation and electrolyte imbalance [36]. The relationship between impaired renal function and MASLD is bidirectional. From one perspective, chronic kidney disease (CKD) may exacerbate liver injury through the release of inflammatory factors and insulin resistance [37]. From another perspective, MASLD-associated lipotoxicity and oxidative stress may directly impair glomerular filtration function [38, 39]. Furthermore, renal insufficiency may limit the efficiency of drug metabolism and increase therapeutic complexity, thus indirectly elevating the risk of death [40]. Consequently, the prognosis of MASLD patients is influenced by these three variables, which affect it from

the perspectives of liver function, exogenous injury, and multi-organ interaction. This suggests that clinical attention should be paid to nutritional support, smoking cessation intervention, and renal function monitoring to improve patient outcomes.

Furthermore, the mortality risk was found to be lower in females than in males. This may be attributable to discrepancies in gender hormones, immune responses, and metabolic pathways [41]. The protective effect of estrogen on the cardiovascular system may partially explain the lower mortality rate observed in women [42]. Additionally, there may be discrepancies in health behaviors and healthcare utilization between genders, which collectively impact the prognosis of MASLD [43]. An increase in age is positively correlated with an elevated mortality risk. As individuals age, their physiological functioning declines, reducing the resilience of multiple organs, including the liver, to disease and stress [44]. Consequently, older patients with MASLD are at an elevated risk of mortality. The mortality rate is significantly higher among smokers than among non-smokers. Patients with hypertension are at an elevated risk of mortality. Hypertension represents a significant risk factor for cardiovascular disease, and it exacerbates MASLD, creating a vicious cycle. Hypertension can exacerbate liver damage, while MASLD may also affect blood pressure control and increase the risk of cardiovascular disease events [45]. A reduction in RBC is associated with an elevated risk

of mortality. A decrease in RBC may be related to anemia, resulting in a diminished capacity to deliver oxygen, affecting body systems' functioning [46]. This is associated with an elevated risk of mortality. Elevated levels of GGT are a significant risk factor for mortality. GGT is predominantly located within the membranes of hepatocytes and microsomes. Consequently, elevated levels of GGT frequently indicate damage to the hepatocytes or bile duct obstruction. In MASLD, elevated GGT levels may reflect the degree of hepatic inflammation and fibrosis, thus serving as an essential marker of poor prognosis [47]. Elevated HbA1c levels have been demonstrated to elevate the risk of mortality significantly. Elevated HbA1c levels indicate suboptimal long-term glycemic control and are associated with an elevated risk of diabetes-related complications, which may include cardiovascular disease, kidney disease, and infections [48].

In conclusion, these nine factors are associated with the pathophysiologic process of MASLD and with patients' overall health status and mortality risk. Incorporating these factors into a prediction model allows for a more comprehensive mortality risk assessment in patients with MASLD, thereby supporting clinical decision-making. In clinical practice, it is essential to consider the variability of these factors to develop personalized treatment and management strategies that can effectively reduce the risk of mortality in patients.

This study additionally generated a nomogram to facilitate the practical application of the intricate statistical findings. The tool's intuitive graphical interface allows clinicians to rapidly and accurately assess the predictive risk of MASLD patients by demonstrating the impact of different factors on their survival probability. This individualized approach to risk assessment can assist in guiding clinical decision-making and facilitating the implementation of early interventions, thereby reducing all-cause mortality in patients with MASLD. To guarantee the precision and dependability of the prediction model, this study employed a range of techniques, including ROC curves, calibration curves, and DCA curves, for performance validation. The results demonstrated that the model AUC values for the training and validation cohorts were approximately 0.85, which is typically regarded as a highly accurate indicator in medical prediction models. Furthermore, calibration and DCA curves were employed to validate the predictive accuracy and generalizability of the models. Moreover, the Kaplan–Meier subgroup analysis of survival curves revealed that males, smokers, and hypertensive patients exhibited a poorer prognosis, with a notable decline in survival probability over time. These findings underscore the significant impact of gender, smoking status, and hypertension on all-cause mortality in patients with MASLD. These

findings support the model's validity in predicting long-term survival probability and provide a foundation for further clinical applications.

The findings of this study have significant implications for the clinical management of patients with MASLD. Firstly, clinicians should stratify risk based on non-modifiable factors such as gender and age and implement interventions for modifiable factors (e.g., smoking, hypertension, glycemic control, etc.) to reduce the risk of death. Secondly, it is recommended that patients at high risk, such as those with low RBC counts, low albumin levels, or high GGT, HbA1c, and creatinine levels, should be monitored more closely and receive active therapeutic interventions. Moreover, the predictive outcomes of the model can serve as a foundation for patient education, enhancing patients' comprehension of the disease's gravity and facilitating the development of a healthful lifestyle. In addition, the present model demonstrated a marked enhancement in the prediction of all-cause mortality when compared with FIB-4 and TyG index, a feat accomplished by integrating demographic, metabolic, and hepatic and renal function indicators across multiple dimensions. Although the present model did not directly incorporate non-invasive indicators of liver fibrosis, such as FIB-4, it indirectly reflected the synergistic effect of liver fibrosis and systemic metabolic disorders through indicators like GGT and albumin. In clinical practice, it is recommended to use the present model in combination with FIB-4: FIB-4 is used for initial screening of liver fibrosis, while the present model is used for comprehensive risk assessment of all-cause mortality.

While the findings of this study are encouraging, it is essential to acknowledge the remaining limitations. First, as the data were derived from a cross-sectional survey, it was impossible to completely exclude the effects of potential temporal bias and confounding factors. A noteworthy constraint of this study is the potential for selection bias resulting from missing data and variable follow-up duration. It would be beneficial for future studies to consider utilizing a prospective cohort design to validate the predictive ability of the model further. Secondly, although the NHANES database is broadly representative, further validation is required to ascertain the applicability of the results of this study in different populations. Thirdly, due to the absence of long-term follow-up liver imaging data (e.g., ultrasound or elastography) in multiple cycles of the NHANES database, incorporating imaging data into the prediction model was not feasible. Furthermore, as our understanding of the pathogenesis of MASLD deepens and new technologies emerge, future studies may consider incorporating additional potential risk factors, such as genetic markers and changes in intestinal flora, to construct a more accurate and comprehensive prediction

model. Ultimately, the efficacy of the prediction model developed in this study in actual clinical practice still requires further observation and evaluation.

Conclusions

In conclusion, the all-cause mortality prediction model developed in this study offers a novel scientific instrument for the clinical supervision of patients with MASLD. This study contributes to the epidemiologic study of MASLD by identifying key predictors and providing valuable information for clinical decision-making. While the study has limitations, its findings point the way forward for future research and clinical practice. They are expected to play an essential role in improving the prognosis of MASLD patients.

Acknowledgements

We thank the NHANES participants and staff for their contributions.

Author contributions

Conceptualization and methodology, project administration, data curation, and investigation, F.Z., L.L., and W.L.; formal analysis, visualization and supervision, W.L.; Writing—original draft, F.Z.; Writing—review and editing, W.L.; funding acquisition, F.Z.; All authors have read and agreed to the published version of the manuscript.

Funding

This work was supported by the Science and Technology Project of Changzhou (CJ20243023) and the Key Talents Project of Changzhou Third People's Hospital.

Availability of data and materials

The National Health and Nutrition Examination Survey dataset is publicly available at the National Center for Health Statistics of the Centers for Disease Control and Prevention (<https://www.cdc.gov/nchs/nhanes/index.htm>).

Declarations

Ethics approval and consent to participate

The studies involving humans were approved by the National Center for Health Statistics Ethics Review Board. The studies were conducted in accordance with the local legislation and institutional requirements. The participants provided their written informed consent to participate in this study.

Consent for publication

Not applicable.

Competing interests

The authors declare no competing interests.

Author details

¹Department of Endocrinology, Changzhou Third People's Hospital, Changzhou 213001, China. ²Department of Clinical Nutrition, Changzhou Third People's Hospital, Changzhou 213001, China. ³Department of Liver Diseases, Changzhou Third People's Hospital, Changzhou 213001, China. ⁴Department of Urology, Changzhou Third People's Hospital, Changzhou 213001, China. ⁵Changzhou Clinical College, Xuzhou Medical University, Changzhou 213001, China.

Received: 17 September 2024 Accepted: 2 May 2025

Published online: 20 May 2025

References

1. Tesfai K, Pace J, El-Newihi N, Martinez ME, Tincopa M, Loomba R. Disparities for hispanic adults with metabolic dysfunction-associated steatotic liver disease in the US: a systematic review and meta-analysis. *Clin Gastroenterol Hepatol*. 2024;23(2):236–49.
2. Chandrasekaran P, Weiskirchen R. The signaling pathways in obesity-related complications. *J Cell Commun Signal*. 2024;18(2): e12039.
3. Zhou XD, Targher G, Byrne CD, Somers V, Kim SU, Chahal CAA, et al. An international multidisciplinary consensus statement on MAFLD and the risk of CVD. *Hepatol Int*. 2023;17(4):773–91.
4. Miao L, Targher G, Byrne CD, Cao YY, Zheng MH. Current status and future trends of the global burden of MASLD. *Trends Endocrinol Metab*. 2024;35(8):697–707.
5. Younossi ZM, Kalligeros M, Henry L. Epidemiology of metabolic dysfunction-associated steatotic liver disease. *Clin Mol Hepatol*. 2025;31(Suppl):S32–S50.
6. Rinella ME, Lazarus JV, Ratziu V, Francque SM, Sanyal AJ, Kanwal F, et al. A multisociety Delphi consensus statement on new fatty liver disease nomenclature. *J Hepatol*. 2023;79(6):1542–56.
7. Rinella ME, Lazarus JV, Ratziu V, Francque SM, Sanyal AJ, Kanwal F, et al. A multisociety Delphi consensus statement on new fatty liver disease nomenclature. *Ann Hepatol*. 2024;29(1): 101133.
8. Riley DR, Hydes T, Hernandez G, Zhao SS, Alam U, Cuthbertson DJ. The synergistic impact of type 2 diabetes and MASLD on cardiovascular, liver, diabetes-related and cancer outcomes. *Liver Int*. 2024;44(10):2538–50.
9. Chen Q, Hu P, Hou X, Sun Y, Jiao M, Peng L, et al. Association between triglyceride-glucose related indices and mortality among individuals with non-alcoholic fatty liver disease or metabolic dysfunction-associated steatotic liver disease. *Cardiovasc Diabetol*. 2024;23(1):232.
10. Targher G, Byrne CD, Tilg H. MASLD: a systemic metabolic disorder with cardiovascular and malignant complications. *Gut*. 2024;73(4):691–702.
11. Hermanson JB, Tolba SA, Chrisler EA, Leone VA. Gut microbes, diet, and genetics as drivers of metabolic liver disease: a narrative review outlining implications for precision medicine. *J Nutr Biochem*. 2024;133: 109704.
12. Li Y, Yang P, Ye J, Xu Q, Wu J, Wang Y. Updated mechanisms of MASLD pathogenesis. *Lipids Health Dis*. 2024;23(1):117.
13. Sawada K, Chung H, Softic S, Moreno-Fernandez ME, Divanovic S. The bidirectional immune crosstalk in metabolic dysfunction-associated steatotic liver disease. *Cell Metab*. 2023;35(11):1852–71.
14. Ran S, Zhang J, Tian F, Qian ZM, Wei S, Wang Y, et al. Association of metabolic signatures of air pollution with MASLD: observational and Mendelian randomization study. *J Hepatol*. 2025;82(4):560–70.
15. Min Y, Wei X, Wei Z, Song G, Zhao X, Lei Y. Prognostic effect of triglyceride glucose-related parameters on all-cause and cardiovascular mortality in the United States adults with metabolic dysfunction-associated steatotic liver disease. *Cardiovasc Diabetol*. 2024;23(1):188.
16. Yin Y, Zhu W, Xu Q. The systemic inflammation response index as a risk factor for hepatic fibrosis and long-term mortality among individuals with metabolic dysfunction-associated steatotic liver disease. *Nutr Metab Cardiovasc Dis*. 2024;34(8):1922–31.
17. Li M, Chen W, Deng Y, Xie W. Impacts of cardiometabolic risk factors and alcohol consumption on all-cause mortality among MASLD and its subgroups. *Nutr Metab Cardiovasc Dis*. 2024;34(9):2085–94.
18. Wang JJ, Zheng Z, Zhang Y. Association of hematological biomarkers of inflammation with 10-year major adverse cardiovascular events and all-cause mortality in patients with metabolic dysfunction-associated steatotic liver disease: the ARIC study. *J Inflamm Res*. 2024;17:4247–56.
19. Center for Disease Control and Prevention Family Questionnaire: Demographic Background/Occupation. 1998. <https://www.cdc.gov/nchs/data/nhanes/public/1999/questionnaires/fq-dm.pdf>. Accessed 29 Mar 2025.
20. Center for Disease Control and Prevention Family Questionnaire: Income. 2000. <https://www.cdc.gov/nchs/data/nhanes/public/1999/questionnaires/fq-in.pdf>. Accessed 29 Mar 2025.
21. Center for Disease Control and Prevention Family Questionnaire: Smoking. 1998. <https://www.cdc.gov/nchs/data/nhanes/public/1999/questionnaires/fq-sm.pdf>. Accessed 29 Mar 2025.
22. Center for Disease Control and Prevention Computer-Assisted Personal Interview (CAPI) Questionnaire: Alcohol. 1998. <https://www.cdc.gov/nchs/data/nhanes/public/1999/questionnaires/calq.pdf>. Accessed 29 Mar 2025.

23. Bedogni G, Bellentani S, Miglioli L, Masutti F, Passalacqua M, Castiglione A, et al. The Fatty Liver Index: a simple and accurate predictor of hepatic steatosis in the general population. *BMC Gastroenterol.* 2006;6:33.
24. Park J, Kim G, Kim BS, Han KD, Kwon SY, Park SH, et al. The associations of hepatic steatosis and fibrosis using fatty liver index and BARD score with cardiovascular outcomes and mortality in patients with new-onset type 2 diabetes: a nationwide cohort study. *Cardiovasc Diabetol.* 2022;21(1):53.
25. Cao C, Cade WT, Li S, McMillan J, Friedenreich C, Yang L. Association of balance function with all-cause and cause-specific mortality among US adults. *JAMA Otolaryngol Head Neck Surg.* 2021;147(5):460–8.
26. Kawanaka M, Nishino K, Ishii K, Tanikawa T, Urata N, Suehiro M, et al. Combination of type IV collagen 7S, albumin concentrations, and platelet count predicts prognosis of non-alcoholic fatty liver disease. *World J Hepatol.* 2021;13(5):571–83.
27. Sheinenzon A, Shehadeh M, Michelis R, Shaoul E, Ronen O. Serum albumin levels and inflammation. *Int J Biol Macromol.* 2021;184:857–62.
28. Daujat-Chavanieu M, Kot M. Albumin is a secret factor involved in multidirectional interactions among the serotonergic, immune and endocrine systems that supervises the mechanism of CYP1A and CYP3A regulation in the liver. *Pharmacol Ther.* 2020;215: 107616.
29. Pennisi G, Pipitone RM, Enea M, De Vincentis A, Battaglia S, Di Marco V, et al. A genetic and metabolic staging system for predicting the outcome of nonalcoholic fatty liver disease. *Hepatol Commun.* 2022;6(5):1032–44.
30. Zhou Z, Park S, Kim JW, Zhao J, Lee MY, Choi KC, et al. Detrimental effects of nicotine on thioacetamide-induced liver injury in mice. *Toxicol Mech Methods.* 2017;27(7):501–10.
31. Ivey R, Desai M, Green K, Sinha-Hikim I, Friedman TC, Sinha-Hikim AP. Additive effects of nicotine and high-fat diet on hepatocellular apoptosis in mice: involvement of caspase 2 and inducible nitric oxide synthase-mediated intrinsic pathway signaling. *Horm Metab Res.* 2014;46(8):568–73.
32. Messner B, Bernhard D. Smoking and cardiovascular disease: mechanisms of endothelial dysfunction and early atherogenesis. *Arterioscler Thromb Vasc Biol.* 2014;34(3):509–15.
33. Gallucci G, Tartarone A, Leroise R, Lalinga AV, Capobianco AM. Cardiovascular risk of smoking and benefits of smoking cessation. *J Thorac Dis.* 2020;12(7):3866–76.
34. Ishida M, Sakai C, Kobayashi Y, Ishida T. Cigarette smoking and atherosclerotic cardiovascular disease. *J Atheroscler Thromb.* 2024;31(3):189–200.
35. Wei Y, Hägg S, Mak JKL, Tuomi T, Zhan Y, Carlsson S. Metabolic profiling of smoking, associations with type 2 diabetes and interaction with genetic susceptibility. *Eur J Epidemiol.* 2024;39(6):667–78.
36. Pottel H, Delanaye P, Cavalier E. Exploring renal function assessment: creatinine, cystatin C, and estimated glomerular filtration rate focused on the european kidney function consortium equation. *Ann Lab Med.* 2024;44(2):135–43.
37. Pan Z, Alqahtani SA, Eslam M. MAFLD and chronic kidney disease: two sides of the same coin? *Hepatol Int.* 2023;17(3):519–21.
38. Wang TY, Wang RF, Bu ZY, Targher G, Byrne CD, Sun DQ, et al. Association of metabolic dysfunction-associated fatty liver disease with kidney disease. *Nat Rev Nephrol.* 2022;18(4):259–68.
39. Bilson J, Mantovani A, Byrne CD, Targher G. Steatotic liver disease, MASLD and risk of chronic kidney disease. *Diabetes Metab.* 2024;50(1): 101506.
40. Verbeeck RK, Musuamba FT. Pharmacokinetics and dosage adjustment in patients with renal dysfunction. *Eur J Clin Pharmacol.* 2009;65(8):757–73.
41. Blum A. Gender differences in vascular aging and in coronary artery disease pathophysiology. *QJM.* 2023;116(9):745–9.
42. Ashraf H, Ashfaq H, Ashraf A. Gender and racial disparities in obesity-related cardiovascular-induced mortality in the USA, 1999–2020. *Curr Probl Cardiol.* 2024;49(1 Pt C):102178.
43. Rogers RG, Everett BG, Onge JM, Krueger PM. Social, behavioral, and biological factors, and sex differences in mortality. *Demography.* 2010;47(3):555–78.
44. Feng Y, Xu W, Tang S, Ye Z, Fang P, Abdullah G, et al. Inflammation, nutrition, and biological aging: The prognostic role of Naples prognostic score in nonalcoholic fatty liver disease outcomes. *Diabetes Res Clin Pract.* 2024;213: 111749.
45. Ng CH, Wong ZY, Chew NWS, Chan KE, Xiao J, Sayed N, et al. Hypertension is prevalent in non-alcoholic fatty liver disease and increases all-cause and cardiovascular mortality. *Front Cardiovasc Med.* 2022;9: 942753.
46. Ren H, Li H, Deng G, Wang X, Zheng X, Huang Y, et al. Severe anemia is associated with increased short-term and long-term mortality in patients hospitalized with cirrhosis. *Ann Hepatol.* 2023;28(6): 101147.
47. Grob SR, Suter F, Katzke V, Rohmann S. The association between liver enzymes and mortality stratified by non-alcoholic fatty liver disease: an analysis of NHANES III. *Nutrients.* 2023;15(13):3063.
48. Wongtrakul W, Charatcharoenwittaya N, Charatcharoenwittaya P. Metabolic dysfunction-associated steatotic liver disease and the risk of mortality in individuals with type 2 diabetes: a systematic review and meta-analysis. *Eur J Gastroenterol Hepatol.* 2024;36(4):351–8.

Publisher's Note

Springer Nature remains neutral with regard to jurisdictional claims in published maps and institutional affiliations.